

Dental Shade Matching Method Based on Hue, Saturation, Value Color Model with Machine Learning and Fuzzy Decision

Shih-Lun Chen,¹ He-Sheng Zhou,¹ Tsung-Yi Chen,¹ Tsung-Han Lee,¹
Chiung-An Chen,^{2*} Ting-Lan Lin,³ Nung-Hsiang Lin,⁴ Liang-Hung Wang,⁵
Szu-Yin Lin,⁶ Wei-Yuan Chiang,² Patricia Angela R. Abu,⁷ and Ming-Yi Lin⁸

¹Department of Electronic Engineering, Chung Yuan Christian University, Taoyuan City 320, Taiwan, ROC

²Department of Electrical Engineering, Ming Chi University of Technology, New Taipei City 301, Taiwan, ROC

³Department of Electronic Engineering, National Taipei University of Technology, Taipei 106, Taiwan, ROC

⁴Department of General Dentistry, Chang Gang Memorial Hospital, Taoyuan City 330, Taiwan, ROC

⁵Department of Microelectronics, College of Physics and Information Engineering,
Fuzhou University, Fuzhou City 350108, China

⁶Department of Computer Science and Information Engineering, National Ilan University,
Yilan County 260, Taiwan, ROC

⁷Department of Information Systems and Computer Science, Ateneo de Manila University,
Quezon City, Philippines

⁸Department of Electrical Engineering, National United University, Miaoli 36003, Taiwan, ROC

(Received February 29, 2020; accepted September 9, 2020)

Keywords: dental shade matching, new fuzzy decision, chrominance, HSV, PSNR, CPSNR, S-CIELAB, SSIM

Color information is an important indicator of color matching. It is recommended to use hue (H) and saturation (S) to improve the accuracy of color analysis. The proposed method for dental shade matching in this study is based on the hue, saturation, value (HSV) color model. To evaluate the performance of the proposed method in matching dental shades, peak signal-to-noise ratio (PSNR), structural similarity index (SSIM), composite peak signal-to-noise ratio (CPSNR), and S-CIELAB (Special International Commission on Illumination, L^* for lightness, a^* from green to red, and b^* from blue to yellow) were utilized. To further improve the performance of the proposed method, dental image samples were multiplied by the weighted coefficients derived by training the model using machine learning to reduce errors. Thus, the PSNR of 97.64% was enhanced to 99.93% when applied with the proposed fuzzy decision model. Results show that the proposed method based on the new fuzzy decision technology is effective and has an accuracy of 99.78%, which is a significant improvement of previous results. The new fuzzy decision is a method that combines the HSV color model, PSNR(H), PSNR(S), and SSIM information, which are used for the first time in research on tooth color matching. Results show that the proposed method performs better than previous methods.

*Corresponding author: e-mail: joannechen@mail.mcut.edu.tw
<https://doi.org/10.18494/SAM.2020.2848>

1. Introduction

The techniques of big data analysis and machine learning are used widely in medicine [detecting pneumonia,⁽¹⁾ autism,⁽²⁾ and risk of falling,⁽³⁾ the classification of cancers,⁽⁴⁾ and the analysis of cell pseudo-color images⁽⁵⁾]. A method of dental image analysis is developed in this study. The classification of dental shade was previously reported in Refs. 6–8, and a further study on dental shade analysis is presented in this study.

Most well-known algorithms use machine learning for training and classification. Guo *et al.*⁽⁹⁾ proposed adaptive mask training for vehicle detection with an assistive system for intelligent transportation. In the system, to improve traffic flow, it is easier to study traffic flow using trained data. Moreover, when a feature vector is compromised and used to store biometric information, through deep learning, a machine-learning-based biometric recognition system can ensure accurate results. Yang *et al.*⁽¹⁰⁾ utilized edge devices that reduce latency and achieved real-time data services in Internet-of-Things (IoT) systems. In healthcare system development, the diagnosis of specific malignancies uses artificial intelligence (AI) techniques to classify symptoms and distinguish whether samples are clean or infected.⁽¹¹⁾ The results are classified on the basis of promise training and may enable the diagnosis of lymph node malignancy in clinical trials. On the other hand, a widely used application of recognition in biometrics is fingerprint detection. Hsia⁽¹²⁾ used binary robustness as a feature of finger vein recognition as a new verification strategy. Finger veins were shown to be a much more stable feature than other biometrics that cannot be copied or stolen.

A small number of people were chosen to receive a new set of teeth, tooth filling, tooth whitening, and other dental surgeries. For teenagers and middle-aged people, a good set of teeth seems to be particularly important. As a result, helping dental patients find the right denture color has become important and necessary. The skill of dentists to accurately determine the right denture color for patients is one of the major factors for patients to consider during denture making. At present, most dentists still use artificial tooth samples as a way for patients to determine the denture ratio by comparing the color of the artificial tooth samples with that of native teeth. A dental plate is used as the standard reference to easily determine the color that matches the natural tooth color.

To determine the tooth color, dentists often compare tooth color labels.^(13,14) However, color swatches do not completely cover the distribution range of the natural color shade of a human tooth. Most palettes lack a series of darker red and yellow colors. Moreover, because of the natural tooth color variability and continuous 3D space of the color distribution, a color block cannot contain all the colors in each color range. If the color difference between the real tooth color and the tooth color tab is within the same range, the difference cannot be distinguished by the human eye and the requirements for practical applications can be met.^(14,15) The VITA classical color cards are currently being used as the standard in the dental market. Figure 1 shows the VITA classical color cards, Vita Zahnfabrik,⁽¹⁶⁾ and its product-based Vitapan 3D-Master color guide.^(17,18)

However, the use of these color cards often causes disputes between dentists and patients because the process involved in producing the actual artificial tooth results in a difference

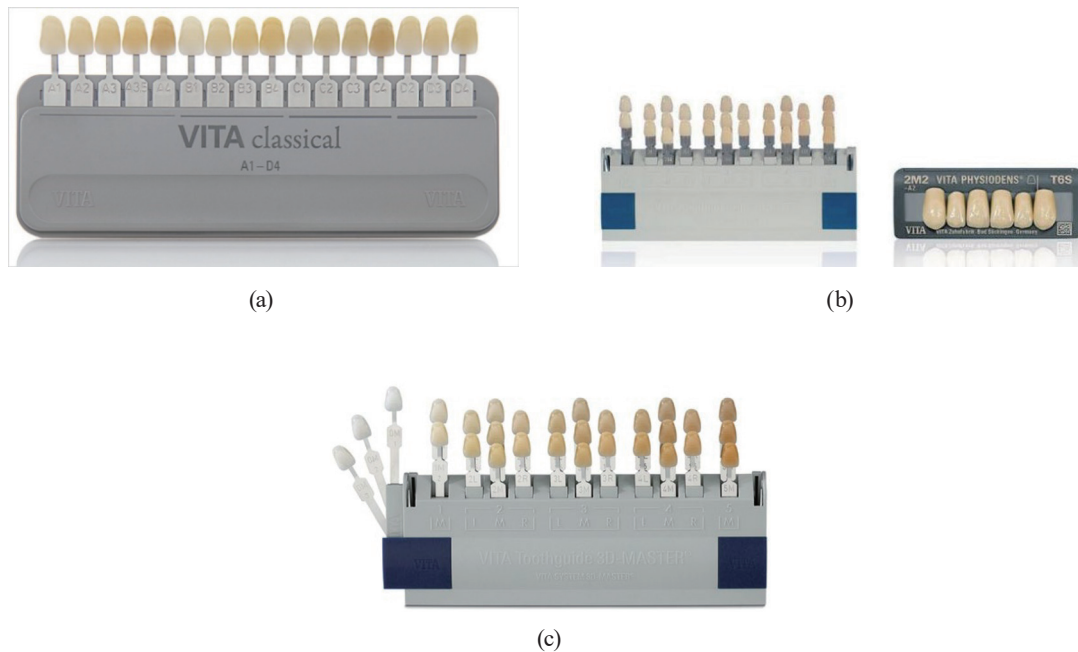


Fig. 1. (Color online) (a) VITA classical color cards,⁽¹⁰⁾ (b) Vita Zahnfabrik,⁽¹⁶⁾ and (c) VITA 3D-Master color guide.^(17,18)

between its final color and the color swatches used in color selection. Moreover, the eyes of a dentist may be fatigued after working long hours, thereby reducing the accuracy of color matching. Furthermore, factors such as light, age, mood, and fatigue can also cause discrepancy in the resulting actual color.⁽¹⁹⁾ All of these factors will negatively affect the color matching results. As such, an effective color analysis method based on the HSV color model for color processing and a new fuzzy decision making method is proposed.

To avoid the above-mentioned problems caused by manual judgment, we propose an image processing technique for color matching. For standard dental colorimetric images, a digital camera is used to create a picture library of the VITA 3D-Master shadow tab, as shown in Fig. 1. Typical resulting images of the captured color chart are shown in Fig. 2. The color of the denture can be determined by comparing the real tooth sample with the color samples in the colorimeter to attain a more accurate match.

2. Literature Review

Algorithms for automatically matching the color of teeth using image processing have been proposed.^(20,21) First, color correction is applied to different images. The system that decides on the color matching analyzes the image of the color card captured with a digital camera.⁽²²⁾ Because the tooth surface is measured with a different device, a color map or average color is necessary. Both the reproduction and verification of shade are needed in the analysis to carry out color matching in the dental clinic.⁽²³⁾ A camera calibration model that includes the Spatial CIELAB (S-CIELAB) method was proposed in Refs. 24 and 25. Using the big data to obtain

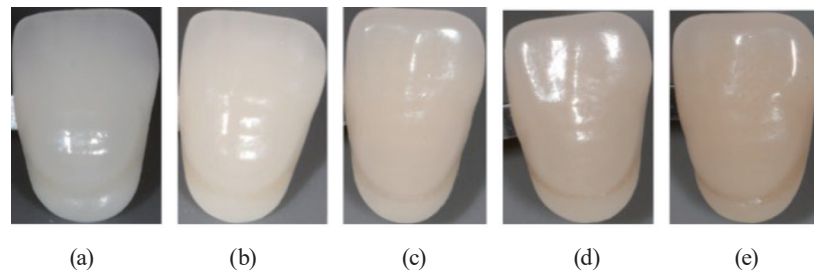


Fig. 2. (Color online) Five shade tab photos of VITA 3D-Master color guide: (a) 1M1, (b) 2M1, (c) 3M1, (d) 4M1, and (e) 5M1.

the required accuracy is the key point to increase the accuracy of all the results.⁽²⁶⁾ The method of computer-aided image processing uses S-CIELAB⁽²⁷⁾ as a classification indicator and was proposed in Ref. 28. Furthermore, a structural similarity index (SSIM) comparison module⁽²⁸⁾ has been used to analyze hue, saturation, value (HSV) colors. Statistical issues in big data regarding values and attributes have been observed. The regression modelling with basic inference procedures, the aspects of model adequacy confirmation, and polynomial regression models and their variations have been investigated.⁽²⁹⁾ Attempts to establish or identify related dependent or independent values have been presented in Ref. 30. The mathematical expressions for modeling the behavior of random variables have been derived. Furthermore, one variable in the linear modeling of the regression results has been found to be used frequently.

Lin *et al.*⁽³¹⁾ proposed a new program for analyzing colorimetric tooth color matching using peak signal-to-noise ratio (PSNR) and a fuzzy decision method. The results indicated an improved accuracy of 92.31%, which is significantly higher than the accuracy of only 32.69% of previous methods. The fuzzy decision method has a higher accuracy and a higher score than the PSNR standard method. Furthermore, this matching method is consistently much better than the traditional method used by dentists. As such, the basis of the matching color method⁽³¹⁾ techniques, specifically linear regression, have been widely used because of their simplicity and effectiveness. In machine learning, a classifier is trained using the defined features. In particular, the accuracy is always the key component of analysis. The improved accuracy in tooth color matching⁽³²⁾ confirmed the validity of the use of the color template with four measured values. Digital images of the samples were taken from digital cameras with color accuracy. Wee *et al.*⁽³³⁾ used various calibration models for the dental color matching of the 264 color patches and 65 shade tabs.

Labeling with a certain accuracy is necessary to calculate the required weighting coefficients, which are examined while training and testing the classifier. To attain the exactness of the classifier, appropriate features and sufficient data are chosen to train a specific set. In addition, the accuracy of the classifier is relative to the amount of data provided to the classifier and the number of selected attributes. The images of the tooth are first converted to the HSV color system representation.⁽³⁴⁾ Different color layers of the HSV have been analyzed using the matching criteria of the PSNR, composite peak signal-to-noise ratio (CPSNR), SSIM, and S-CIELAB. Y'CbCr can be used to optimize the transmission of color signals. Here, Y stands for brightness or luminosity, which is a grayscale value; Cb and Cr stand for

blue and red density offset components, respectively. Therefore, this approach is backward-compatible with monochrome television, which is entirely black and white. Furthermore, three independent video signals are transmitted simultaneously using the RGB color model. We provide the benefits of reduced transmission data and a smaller bandwidth used by the methods of saturating images and specified pixels in colors. Thus, the HSV color system is similar to visual judgment, but the combination of HSV and machine learning results in a huge improvement.

3. Proposed Methodology

3.1 Image acquisition

A digital camera is used to obtain pictures of each VITA 3D-Master shade tab.⁽³⁴⁾ It is ensured that the environment while capturing photos of each tab simulates the actual conditions of the dentist assisting the patients during the matching of tooth color. Two photos are taken to generate two sets of images for the test datasets, namely, datasets A and B. A colorimetric analysis is then performed on these two datasets to label each photo, and the photos are arranged in the same order as those of the VITA 3D-Master shade tabs. Each dataset includes 26 tagged photos with depths of 24 bits per pixel and 8 bits for each of the R, G, and B color values. The average size of the images in the dataset is 360×520 pixels.

Figure 3 shows the flowchart of the proposed tooth color matching algorithm. There are four main steps: color photo preprocessing, criteria evaluation, the addition of parameters for weighting coefficients, and fuzzy decision.

Step 1: Preprocessing of color photos

Normalization is applied to the raw images to adjust the pixel intensity range. The extension of the dynamic range is the main idea of standardization. This standardization brings the

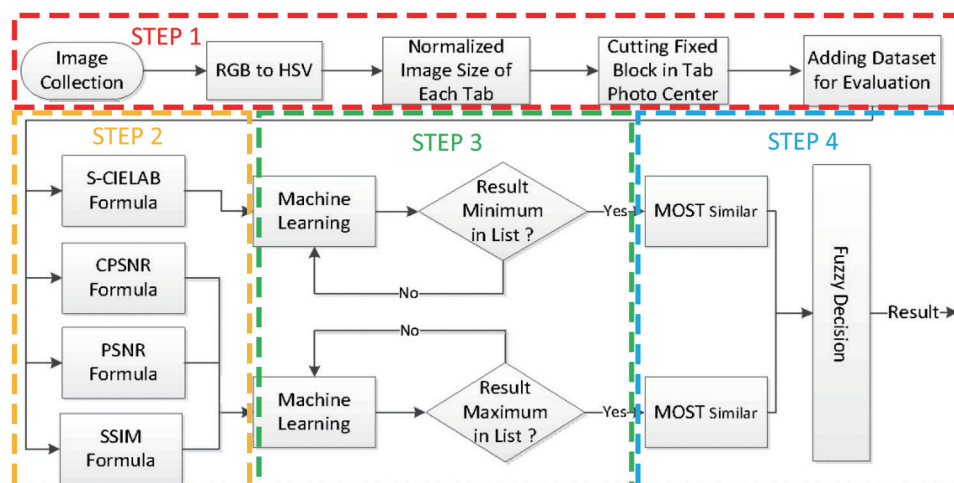


Fig. 3. (Color online) Flowchart of the proposed dental shade matching algorithm.

image into a range of normalized values to avoid diagnosis error. The image file should be normalized to a format that includes the whole dynamic range of the digital blocks specified. After the standardization, the photo is segmented to remove unnecessary items from the standardized features. Furthermore, the segmentation is fixed by changing one aspect ratio to another without stretching the image. After these preprocessing steps, the images must be evaluated while using the dataset to ensure the completeness of data. The S-CIELAB, CPSNR, and PSNR formulas are captured from an image obtained using a digital camera. As such, the original image is stored in an RGB format. Accordingly, the substep pertaining to the format is the conversion of the RGB image to the HSV format, which is advantageous since it simplifies the colorimetric analysis. Equations (1)–(3) show the conversion from the RGB format to the HSV format.

$$H = \cos^{-1} \left(\frac{\frac{1}{2}2R - G - B}{R - G^2 - R - GB - B} \right) \quad (1)$$

$$S = \frac{\max\{R, G, B\} - \min\{R, G, B\}}{\max\{R, G, B\}} \quad (2)$$

$$V = \max\{R, G, B\} \quad (3)$$

Each tooth photo is then scaled to a fixed size of 300×500 pixels, followed by the segmentation of the length and width of the photo to 50 to 250 pixels. As shown in Fig. 4, the scaled image is used for comparison with other data sets. The scaling and cutting process is part of the normalization of the size of the tooth images. Consequently, the accuracy of the colorimetric analysis is improved.

Step 2: Evaluation of criteria

The captured images in datasets A and B were obtained using the same VITA 3D-Master shade tabs. Therefore, these two datasets are compared by different tooth color matching methods to determine the matching accuracies of the methods. When the target photo in one

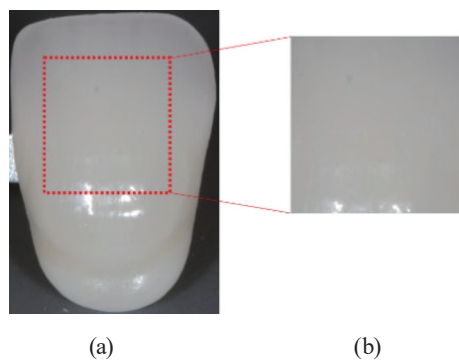


Fig. 4. (Color online) (a) Original image and (b) the normalized and cut region of the image.

dataset is matched with the corresponding photo in the other dataset by the tooth color matching method, matching is considered correct. When the dental color matching method identifies a photo that does not correspond to the target, matching is considered incorrect. The two datasets are used to evaluate the performance characteristics of the different tooth color matching methods.

There are four evaluation criteria that are used in the proposed algorithm. The first criterion is the S-CIELAB of the HSV image, which is a measure of the color difference. A small S-CIELAB value indicates that the colors of the two images are highly similar. Therefore, the first evaluation criterion is to select the tooth image with the smallest S-CIELAB value. The second and third criteria respectively concern the H (hue) and S (saturation) values of the PSNR criterion of the tooth image. The higher the PSNR, the higher the color similarity. The fourth criterion is the SSIM standard, which is used to evaluate the similarity of the dental image structure. In terms of image measurement, it is consistent with the judgment of the image by the human eyes. As such, the higher the SSIM, the more similar are the images. Finally, the target image will be selected on the basis of the smallest S-CIELAB value, the highest SSIM, and the highest H and S PSNRs. Once determined, the module for the weighting coefficients of parameters is set.

3.2 Image evaluation criteria

S-CIELAB⁽³⁵⁾

In previous studies,^(32,34) ΔE_{ab}^* in S-CIELAB was used, and the color difference was applied individually to a single uniform color patch. This is based on the concept of spatial distribution. A smaller S-CIELAB value implies that the images are more closely related and have smaller distortions. The S-CIELAB ΔE_{ab}^* can be calculated using Eqs. (4)–(8).

$$\Delta E_{ab}^* = \sqrt{(\Delta L^*)^2 + (\Delta a^*)^2 + (\Delta b^*)^2} \quad (4)$$

$$\Delta L^* = \begin{cases} 116 \left(\frac{Y}{Y_n} \right)^{\frac{1}{3}} - 16 & \text{if } \frac{Y}{Y_n} > 0.008856 \\ 903.3 \left(\frac{Y}{Y_n} \right) & \text{if } \frac{Y}{Y_n} \leq 0.008856 \end{cases} \quad (5)$$

$$a^* = 500 \times \left(f \left(\frac{X}{X_n} \right) - f \left(\frac{Y}{Y_n} \right) \right) \quad (6)$$

$$b^* = 200 \times \left(f \left(\frac{Y}{Y_n} \right) - f \left(\frac{Z}{Z_n} \right) \right) \quad (7)$$

$$f(t) = \begin{cases} \frac{1}{t^3} & \text{if } t > 0.008856 \\ 7.787 \times t + \frac{16}{116} & \text{if } t \leq 0.008856 \end{cases} \quad (8)$$

Here, $X / X_n = Y / Y_n = Z / Z_n$, where X , Y , and Z are the three color values of the object. X_n , Y_n , and Z_n are the three color values of the reference white. Each halftone patch of high visibility is represented by the scanned values of X_n , Y_n , and Z_n . After the prediction of S-CIELAB, the calculation of specifications, and the comparison of halftones, the average field and ΔE values are distributed at average levels.⁽³⁴⁾ Moreover, the values of the original halftone patch for both the pixel and the corresponding pixel are compared with the overall index. The parameter L is 100 times the Munsell brightness; when L is set to 0, the color becomes black, and when it is set to 100, the color becomes white. The parameters a^* and b^* indicate red–green and yellow–blue coordinates, respectively.

CPSNR⁽³⁶⁾

In the general method, the components of the R, G, and B color model are combined to form a colored image. The quality of the resulting image can be evaluated using the CPSNR criterion. In this work, the CPSNR is calculated by combining the components of H, S, and V to form an image, and then it is used for judgment. A larger CPSNR implies a smaller image distortion. The relevant definitions of CPSNR are shown in Eqs. (9)–(11).

$$CPSNR = 10 \times \log_{10} \left(\frac{255^2}{CMSE} \right) \quad (9)$$

$$CMSE = \frac{\sum_{n=1}^{FrameSize} (I_n - P_n)}{FrameSize} \quad (10)$$

$$FrameSize = ImageLength \times ImageWidth \times Number\ of\ channels \ (Grayscale\ is\ 1,\ color\ is\ 3) \quad (11)$$

PSNR⁽³⁷⁾

PSNR values are commonly measured in work on image quality. As shown in Eqs. (12)–(14), the maximum value and error terms in the images are considered for evaluation.

$$PSNR = 10 \times \log_{10} \left(\frac{255^2}{MSE} \right) \quad (12)$$

$$MSE = \frac{\sum_{n=1}^{FrameSize} (I_n - P_n)^2}{FrameSize} \quad (13)$$

$$\text{FrameSize} = \text{ImageLength} \times \text{ImageWidth} \times \text{Number of channels} \text{ (Grayscale is 1, color is 3)} \quad (14)$$

I_n is the n -th pixel value of the original image and P_n is the n -th pixel value of the processed image.

Structural similarity index (SSIM)⁽³⁸⁾

SSIM is an index used to measure the similarity of two digital images. As shown in Eqs. (15) and (16), the maximum value of the image and the error term are considered for evaluation. Because of its simplicity and effectiveness, SSIM has been popularly used in applications related to image and video processing in recent years.

$$\text{SSIM}(x, y) = \frac{(2\mu_x\mu_y + C_1)(2\sigma_{xy} + C_1)}{(\mu_x^2 + \mu_y^2 + C_1)(\sigma_x^2 + \sigma_y^2 + C_2)} \quad (15)$$

$$\text{FrameSize} = \text{ImageLength} \times \text{ImageWidth} \times \text{Number of channels} \text{ (Grayscale is 1, color is 3)} \quad (16)$$

Step 3: Add parameters for weighting coefficients

Draper and Smith⁽³⁰⁾ described a method of obtaining the values and attributes of a problem through a statistical graph. In addition, the dependent and independent variables are identified and analyzed for establishing or identifying existing relationships between them. This procedure is described as linear regression in statistics and is commonly used since it is simple and efficient.

The steps are as follows. First, the analysis of the colorimetric modules of datasets A and B. Second, the appropriate interval weighting coefficients are integrated by linear regression. The coefficients are obtained from experimentally determined evaluation indices. Third, the control interval is adjusted throughout the experiment. The idea is to widen the interval of its judgment values by using the dichotomy, which compares the two adjacent values and marks the close one to simplify the procedure, to easily compare these indices. The dichotomy compares the two adjacent values and marks the close one to simplify the procedure.

Training the modules by applying the values of the colorimetric modules, i.e., SSIM, PSNR(H), and PSNR(S), is acceptable since the weighting factors are required and limited. The valid range of correct ratios is between 1 and 9%. Although the valid range is continuously increasing, the results will be less than expected. PSNR(Hw) and PSNR(Sw) represent the adjusted weights of PSNR(H) and PSNR(S), respectively. Figure 5 shows the scores obtained from the scoring formula of colorimetric modules for dentures with 1 to 9% weight training. Figure 6 shows the correct ratios of dentures obtained using the colorimetric module with 1 to 9% weight training.

Step 4: Fuzzy decision

The fuzzy decision is well known in many fields of studies such as power control⁽³⁹⁾ and prediction.⁽⁴⁰⁾ Gulzard *et al.*⁽⁴¹⁾ provided a fuzzy mapping approach for usability

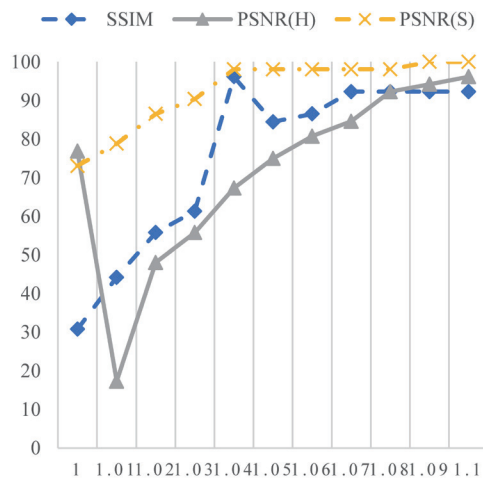


Fig. 5. (Color online) Weight training using datasets A and B.

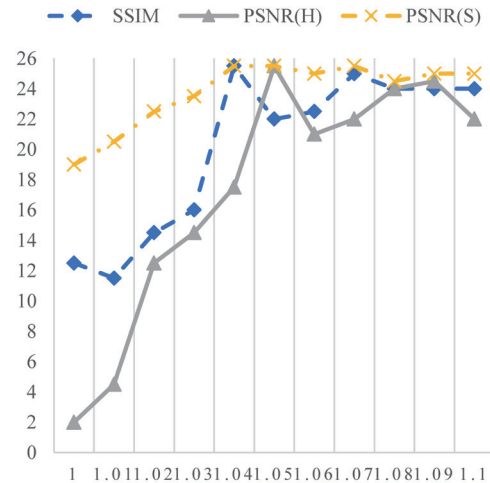


Fig. 6. (Color online) Accuracy after training with datasets A and B.

qualities. For individual photos, the matching photo is determined by adaptive correspondence by the fuzzy decision.⁽⁴²⁾ Additionally, the fuzzy controller seeks high-quality results automatically. The related factors are set to the correct results of the fuzzy processor and simplistically displayed. For example, the proposed method provided the brightness, contrast value, hue, saturation, and environmental parameters, which are found in each tooth detail and are therefore beneficial to controlling the fuzzy decision. The fuzzy decisions based on experimental evaluation⁽⁴³⁾ and fuzzy logic⁽⁴⁴⁾ are well suited for solving problem spaces with partial authenticity. Data mining, the concept of fuzzy logic with classification techniques, is used for processing the uncertainty in a dataset.

A new type of fuzzy decision making that obeys the fundamental rules of machine language was realized⁽⁴⁴⁾ and is applied here to the proposed algorithm to select S-CIELAB, SSIM, PSNR(H), and PSNR(S) for tooth color matching. In the proposed fuzzy decision method, one of the inputs is the brightness of tooth color. The brightness of the tab photo is $b(n)$. The other input is the hue of the tooth color in the tab photo. The chroma of the tab photo is $c(n)$. The lightness $b(n)$ and chroma $c(n)$ are indicated by tab numbers of the VITA 3D-Master color guide. For example, the tab number in Fig. 2(d) is 5M1, which means that $b(n)$ is 5 and $c(n)$ is 1.

On the basis of the expert system, the algorithm is designed to use datasets A and B to calculate each accuracy score induction. Table 1 shows the tooth color matching accomplished using the initial fuzzy adjusted rules. Moreover, the values given in the experimental result section are used for training the adjustment rules for a different fuzzy dataset. On acquiring accuracy and score results, the datasets are used to train the different machine learning datasets listed in the following tables. The scoring results obtained using datasets A and B to train the fuzzy adjustment rules are listed in Table 1. To obtain the results in Table 1, datasets C and D are used as test datasets. With the input fuzzy sets of $b(n)$ and $c(n)$, the fuzzy adjustment rule maps the two features to the output fuzzy set of $o(n)$.

With the use of datasets C and D as test datasets, the accuracy and score results listed in Tables 10–14 were obtained. The fuzzy adjustment rule of the two features, namely, the input

Table 1
Fuzzy adjustment rules for brightness $b(n)$ and chroma $c(n)$.

		$b(n)$						
		XM1	XM2	XM3	XL1.5	XL2.5	XR1.5	XR2.5
$c(n)$	1MX	PSNR (H)	PSNR (H)	—	—	—	—	—
	2MX	PSNR (H)	SSIM	PSNR (H)	SSIM	PSNR (H)	PSNR (H)	PSNR (H)
	3MX	PSNR (H)	S-CIE LAB	PSNR (S)	PSNR (S)	S-CIE LAB	PSNR (S)	S-CIE LAB
	4MX	PSNR (H)	PSNR (V)	PSNR (H)	PSNR (S)	PSNR (S)	PSNR (S)	PSNR (S)
	5MX	PSNR (S)	PSNR (S)	PSNR (S)	—	—	—	—

fuzzy sets of $b(n)$ and $c(n)$, was based on the results of evaluating the criteria of datasets A and B. Their output fuzzy set of $o(n)$ can be mapped. After selecting the best results from the three criteria, each tooth image can be matched with the shadow tab with the highest degree of correspondence. Therefore, the fuzzy logic decision method could effectively improve the accuracy of tooth shadow matching.

4. Experimental Results

The VITA 3D-Master color guide⁽¹⁵⁾ has 26 dental shadow tabs that can be classified on the basis of brightness and chroma information. As shown in Table 1, the classifications of XM1, XM2, XM3, XL1.5, XL2.5, XR1.5, and XR2.5 are based on brightness. On the other hand, the classifications of 1MX, 2MX, 3MX, 4MX, and 5MX are based on chroma. To develop an index to evaluate the accuracy of tooth shadow matching, a scoring formula [Eq. (17)] with values between 0 and 100 is developed to determine the accuracy of tooth shadow matching. The scoring formula considers the effects of brightness and chroma and uses a linear decrement for matching. On the basis of the results in the above processing, the base image in the comparison database and the reference image in the reference dataset have the most relevant chroma values. As such, the comparison score of the reference image is determined as 100. The second-highest correlation can yield the score of the reference image reduced by one by comparing the chroma value of the real image in the dataset. The total number of teeth defined as having the highest score of 100 is divided by 26 (the number of dental shadow tabs) to obtain a gap unit of about 3.8462. Therefore, the score can be calculated as

$$Score = 100 - [3.8462 \times (N - 1)], \quad (17)$$

where N is the ground truth image in the comparison of the dataset, and its chroma value is the most relevant to the N th reference image in the reference dataset. It shows that even if the score is not accurate, it is close to 100. It also represents the different color spaces of each dental shadow tab. For example, if the colorimetric result is correct, the score is 100 points. If the

colorimetric value is the second most relevant, the given score is $100 - 3.8462 = 96.15$ points. If a value is the third smallest, the score is $100 - (3.8462 \times 2) = 92.31$ points and so on.

The method discussed in this section is compared with the existing S-CIELAB method for tooth shadow matching.⁽³²⁾ Table 2 shows the results of S-CIELAB (H, S, V) and S-CIELAB (Y, Cb, Cr)⁽³⁴⁾ with the average score of each reference image in two modes of comparison. The results of CPSNR (H, S, V) and CPSNR (Y, Cb, Cr)⁽³⁰⁾ are given in Table 3. From Tables 2 and 3, it is evident that the accuracy rates of the evaluation, analysis, and screening using the HSV approach of the VITA 3D-Master color guide⁽⁷⁾ are higher than those obtained using Ycber.

To determine the clinical application of this method, this study was carried out in collaboration with Dr. Nung-Hsiang Lin and Dr. Yufang Guo of the Department of General Dentistry of Chang Gang Memorial Hospital. Figure 7 shows a sample of original images of a tooth in datasets A, B, C, and D. Through the use of tooth colorimetric plates and related clinical resources provided by Chang Gang Memorial Hospital, the relevant clinical environment has been restored and constructed, including the tooth ratio in the swatch photographing environment and the ease of capturing the target tooth color and using the color comparison technology proposed in this article. The aim of this study is to develop a technology that can be easily used by dentists to automatically compare tooth colors using the proposed program. This will reduce the time taken for tooth color comparison and finding the appropriate denture color.

Table 2
Scores obtained using S-CIELAB (H, S, V) and (Y, Cb, Cr)⁽²³⁾ criteria.

Reference tab image	S-CIELAB			
	Dataset A compared with dataset B	Dataset B compared with dataset A	Average	Average ⁽³⁴⁾
1M1	100	100	100	100
1M2	100	100	100	100
2M1	76.92	76.92	76.92	40.39
2M2	96.15	96.15	96.15	96.15
2M3	100	96.15	98.08	96.16
2L1.5	100	100	100	100
2L2.5	96.15	96.15	96.15	86.54
2R1.5	96.15	84.62	90.39	73.08
2R2.5	100	96.15	98.08	100
3M1	65.38	84.62	75	53.85
3M2	96.15	80.77	88.46	65.39
3M3	96.15	73.08	84.62	73.08
3L1.5	84.62	100	92.31	96.16
3L2.5	84.62	88.46	86.54	69.23
3R1.5	92.31	100	96.16	86.54
3R2.5	80.77	65.38	73.08	59.62
4M1	88.46	100	94.23	78.85
4M2	80.77	100	90.39	80.77
4M3	96.15	88.46	92.31	75
4L1.5	100	100	100	100
4L2.5	80.77	96.15	88.46	75
4R1.5	61.54	84.62	73.08	59.62
4R2.5	84.62	80.77	82.7	59.62
5M1	34.61	100	67.31	57.7
5M2	76.92	100	88.46	80.77
5M3	100	100	100	100
Average	87.28	91.86	89.57	79.36

Table 3
Scores obtained using CPSNR(H, S, V) and (Y, Cb, Cr)⁽²³⁾ criteria.

Reference tab image	CPSNR			
	Dataset A compared with dataset B	Dataset B compared with dataset A	Average	Average ⁽³⁴⁾
1M1	100	100	100	100
1M2	100	100	100	100
2M1	80.77	80.77	80.77	48.08
2M2	100	100	100	100
2M3	100	100	100	100
2L1.5	100	100	100	100
2L2.5	84.62	82.7	83.66	63.46
2R1.5	100	96.16	98.08	90.39
2R2.5	100	100	100	100
3M1	76.92	82.69	79.81	63.46
3M2	100	86.54	93.27	69.23
3M3	96.15	86.54	91.35	84.62
3L1.5	80.77	90.39	85.58	84.62
3L2.5	84.62	90.39	87.51	86.51
3R1.5	96.15	98.08	97.12	90.39
3R2.5	84.62	76.93	80.78	63.46
4M1	96.15	98.08	97.12	92.31
4M2	80.77	90.39	85.58	94.23
4M3	100	94.23	97.12	92.31
4L1.5	100	100	100	100
4L2.5	88.46	92.31	90.39	90.39
4R1.5	69.23	80.77	75	63.46
4R2.5	84.62	86.54	85.58	63.46
5M1	46.15	73.08	59.62	59.62
5M2	80.77	90.39	85.58	86.54
5M3	100	100	100	100
Average	89.65	91.43	90.53	84.10

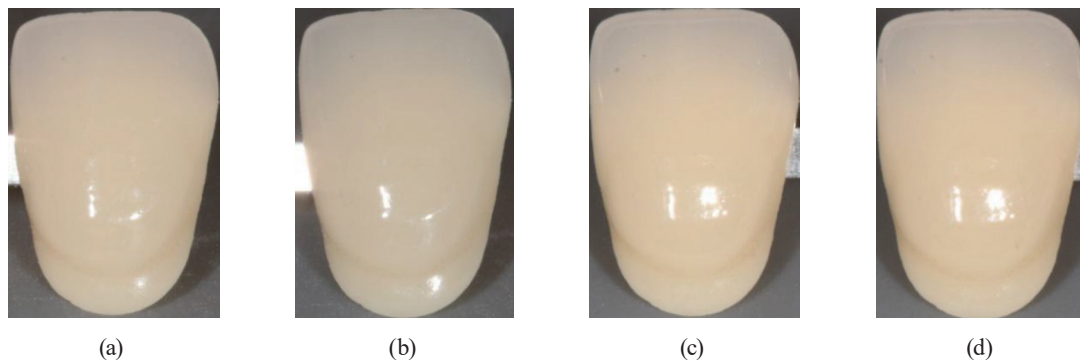


Fig. 7. (Color online) Clinical dental images from Department of General Dentistry in Chang Gang Memorial Hospital. Datasets (a) A, (b) B, (c) C, and (d) D.

The two proposed methods are S-CIELAB and CPSNR. SSIM, PSNR(H), PSNR(S), and fuzzy methods are also used. The values used for training were from datasets A and B. The performance of color matching is evaluated using different criteria. Each dataset has 26 tooth shadow images taken under different conditions. The S-CIELAB⁽²⁴⁾ method was used with the first shadow image in dataset A as a reference. Twenty-six (26) S-CIELAB values were calculated using the 26 tooth shadow images in database B. The S-CIELAB value of the tooth

shadow image in dataset B with the highest correlation (the lowest S-CIELAB value or the highest CPSNR, SSIM or PSNR value) to one tooth shadow image in dataset A is displayed and specified as the correct result. This is done for all 26 tooth shadow images in dataset A. This process is repeated continuously and considered to produce the reference datasets. The number of correct results after comparing dataset A with dataset B is listed in Table 2. Equation (18) is used to compute the accuracy by dividing the number of correctly matched images with the total number of pictures (26 tooth shadow images per dataset).

$$Accuracy = \frac{\text{No. of correct shade matching pictures}}{\text{Total no. of pictures}} \times 100 \quad (18)$$

In Table 3, the comparison accuracies of datasets B and A are listed. The test is repeatedly applied with all the comparison methods described above using the same set of steps with dataset B as the reference for comparing the images in dataset A. Table 4 shows the values of PSNR(V).

Tables 5–7 show the values of SSIM, PSNR(H), and PSNR(S) after machine learning was used to select the best weighting coefficients. The weights (H), (S), and (V) are labeled (Hw), (Sw), and (Vw), respectively.

The results of the fuzzy method show that the accuracy of analysis and screening when using HSV is higher than that when using YcbCr. In addition, the whiter areas of the VITA 3D-Master color guide⁽¹⁵⁾ have a higher accuracy, as listed in Table 8.

Table 4
Scores obtained using PSNR(V) criteria.

Reference image	PSNR(V)		
	Dataset A compared with dataset B	Dataset B compared with dataset A	Average
1M1	11.54	11.54	11.54
1M2	84.62	84.62	84.62
2M1	69.23	53.85	61.54
2M2	100	100	100
2M3	84.62	73.08	78.85
2L1.5	65.38	88.46	76.92
2L2.5	100	92.31	96.16
2R1.5	96.15	100	98.08
2R2.5	84.62	100	92.31
3M1	92.31	92.31	92.31
3M2	88.46	76.92	82.69
3M3	61.54	53.85	57.70
3L1.5	100	100	100
3L2.5	96.15	96.15	96.15
3R1.5	34.61	69.23	51.92
3R2.5	100	100	100
4M1	100	100	100
4M2	96.15	73.08	84.62
4M3	96.15	100	98.08
4L1.5	69.23	100	84.62
4L2.5	76.92	92.31	84.62
4R1.5	88.46	69.23	78.85
4R2.5	92.31	73.08	82.70
5M1	100	100	100
5M2	73.08	96.15	84.62
5M3	88.46	100	94.23
Average	82.69	84.47	83.58

Table 5
Scores obtained using SSIM criteria.

Reference image	SSIM		Average
	Dataset A compared with dataset B	Dataset B compared with dataset A	
1M1	84.62	84.62	84.62
1M2	84.62	84.62	84.62
2M1	96.15	92.31	94.23
2M2	100	100	100
2M3	80.77	96.15	88.46
2L1.5	100	100	100
2L2.5	88.46	69.23	78.845
2R1.5	50	96.15	73.075
2R2.5	61.54	100	80.77
3M1	100	92.31	96.155
3M2	100	65.38	82.69
3M3	100	96.15	98.075
3L1.5	100	100	100
3L2.5	100	100	100
3R1.5	80.77	100	90.385
3R2.5	100	100	100
4M1	69.23	84.62	76.925
4M2	96.15	46.15	71.15
4M3	84.62	100	92.31
4L1.5	26.92	100	63.46
4L2.5	65.38	100	82.69
4R1.5	88.46	100	94.23
4R2.5	100	73.08	86.54
5M1	92.31	100	96.155
5M2	73.08	100	86.54
5M3	84.62	100	92.31
Average	84.91	91.57	88.24

Table 6
Scores obtained using PSNR(Hw) criteria.

Reference image	PSNR(Hw)		Average
	Dataset A compared with dataset B	Dataset B compared with dataset A	
1M1	100	100	100
1M2	100	100	100
2M1	100	100	100
2M2	100	100	100
2M3	100	100	100
2L1.5	100	100	100
2L2.5	100	100	100
2R1.5	100	100	100
2R2.5	100	100	100
3M1	100	100	100
3M2	100	80.77	90.39
3M3	100	100	100
3L1.5	100	100	100
3L2.5	100	100	100
3R1.5	100	100	100
3R2.5	100	100	100
4M1	100	100	100
4M2	100	34.61	67.31
4M3	100	100	100
4L1.5	80.77	100	90.39
4L2.5	80.77	100	90.39
4R1.5	100	100	100
4R2.5	100	100	100
5M1	100	100	100
5M2	100	100	100
5M3	100	100	100
Average	98.52	96.75	97.64

Table 7
Scores obtained using PSNR(Sw) criteria.

Reference image	PSNR(Sw)		Average
	Dataset A compared with dataset B	Dataset B compared with dataset A	
1M1	100	100	100
1M2	100	100	100
2M1	100	100	100
2M2	100	100	100
2M3	100	100	100
2L1.5	100	100	100
2L2.5	100	100	100
2R1.5	100	100	100
2R2.5	100	100	100
3M1	100	100	100
3M2	100	100	100
3M3	100	100	100
3L1.5	100	100	100
3L2.5	100	100	100
3R1.5	100	100	100
3R2.5	100	100	100
4M1	100	100	100
4M2	100	96.15	98.08
4M3	100	100	100
4L1.5	100	100	100
4L2.5	100	100	100
4R1.5	100	100	100
4R2.5	100	100	100
5M1	100	100	100
5M2	100	100	100
5M3	100	100	100
Average	100	99.85	99.93

Table 8
Scores obtained by the fuzzy decision method: (H, S, V) vs (Y, Cb, Cr).⁽³¹⁾

Reference image	Fuzzy			Average ⁽²³⁾
	Dataset A compared with dataset B	Dataset B compared with dataset A	Average	
1M1	100	100	100	100
1M2	100	100	100	100
2M1	100	100	100	100
2M2	100	100	100	100
2M3	100	100	100	100
2L1.5	100	100	100	100
2L2.5	92.31	92.31	92.31	86.54
2R1.5	100	100	100	100
2R2.5	100	100	100	100
3M1	100	100	100	100
3M2	96.15	100	98.08	88.46
3M3	100	100	100	100
3L1.5	100	100	100	92.31
3L2.5	100	100	100	100
3R1.5	100	100	100	100
3R2.5	100	100	100	100
4M1	100	100	100	100
4M2	100	96.15	98.08	100
4M3	100	100	100	100
4L1.5	100	100	100	100
4L2.5	100	100	100	100
4R1.5	100	100	100	100
4R2.5	84.62	100	92.31	100
5M1	100	100	100	100
5M2	100	100	100	100
5M3	100	100	100	100
Average	98.96	99.56	99.26	98.74

Tables 9 and 10 show the corresponding results obtained using dataset B as the reference for comparing dataset A. Furthermore, a statistical method was developed on the basis of the submechanism to standardize the results. Consequently, the results of comparison could be examined in greater detail. Another comparison is performed and the results obtained are listed as scores of machine learning of SSIM and numbers of accurate shade matching pictures. The colorimetric is decided by the purposed algorithm to find out the most closed color of the original tooth color. The goal for this current comparison is to simplify this binary result and show any intermediate trend of inaccuracy.

At the beginning of the experiment, the weight of PSNR(Hw) had a markedly wide color range. To optimize the comparison accuracy, the trial-and-error method may provide a smaller color range. In the following methods, weights in the range from $W = 1.0$ to 1.1 were used for the dataset images. On the other hand, integrating machine learning enabled the determination

Table 9
(H, S, V) vs (Y, Cb, Cr).⁽²³⁾ Numbers of exact shadow matching pictures obtained by different methods.

	SCIELAB (Y,Cb,Cr) ⁽²⁷⁾	CPSNR (Y,Cb,Cr) ⁽²⁷⁾	Fuzzy decision (Y,Cb,Cr) ⁽²⁷⁾	SCIELAB (H,S,V)	CPSNR (H,S,V)	Fuzzy decision
Dataset A compared with dataset B	20	21	24	18	19	23
Dataset A compared with dataset B	7	8	24	22	20	24

Table 10
Scores obtained using PSNR(Hw) machine learning criteria.

Reference image	PSNR(Hw)									
	Dataset A compared with dataset B ($W = 1.08$)	Dataset B compared with dataset A ($W = 1.08$)	Dataset A compared with dataset B ($W = 1.06$)	Dataset B compared with dataset A ($W = 1.06$)	Dataset A compared with dataset B ($W = 1.07$)	Dataset B compared with dataset A ($W = 1.07$)	Dataset A compared with dataset B ($W = 1.09$)	Dataset B compared with dataset A ($W = 1.09$)	Dataset A compared with dataset B ($W = 1.1$)	Dataset B compared with dataset A ($W = 1.1$)
	1M1	100	100	100	100	100	100	100	100	100
1M2	100	100	100	100	100	88.46	100	92.31	100	100
2M1	100	100	84.62	84.62	100	100	100	100	57.69	57.69
2M2	100	100	100	100	46.15	100	53.85	100	100	100
2M3	100	100	100	100	100	100	100	100	100	100
2L1.5	100	100	100	100	80.77	100	84.62	100	100	100
2L2.5	100	100	100	100	100	100	100	100	100	100
2R1.5	100	100	100	100	100	100	100	100	69.23	100
2R2.5	100	100	100	100	100	100	100	100	92.31	100
3M1	100	100	100	100	100	80.77	100	84.62	100	100
3M2	100	80.77	61.54	61.54	100	34.61	100	42.31	100	53.85
3M3	100	100	100	100	100	100	100	100	100	100
3L1.5	100	100	100	100	42.31	100	42.31	100	100	100
3L2.5	100	100	100	100	100	100	100	100	100	100
3R1.5	100	100	100	100	100	100	100	100	80.77	100
3R2.5	100	100	100	100	100	100	100	100	100	100
4M1	100	100	96.15	96.15	96.15	100	100	100	100	38.46
4M2	100	34.61	23.08	23.08	100	100	100	100	100	19.23
4M3	100	100	100	100	100	80.77	100	84.62	100	100
4L1.5	80.77	100	100	100	100	100	100	100	42.31	100
4L2.5	80.77	100	53.85	100	100	100	100	100	42.31	100
4R1.5	100	100	100	100	100	100	100	100	76.92	100
4R2.5	100	100	100	100	100	100	100	100	100	96.15
5M1	100	100	100	100	100	100	100	100	100	100
5M2	100	100	80.77	100	100	100	100	100	80.77	100
5M3	100	100	100	100	100	100	100	100	76.92	100
Average	98.52	96.75	92.31	94.82	94.82	95.56	95.41	96.3	89.2	90.98

of the best weight for PSNR(Hw), $W = 1.08$. The accuracy in the comparison of dataset A with dataset B can reach up to 98.52%. To verify this as the best accuracy, weights of $W = 1.06, 1.07, 1.09$, and 1.1 were examined and the results are listed in Table 10. The results obtained with $W = 1.07$ and 1.09 are very close to that obtained with $W = 1.08$. Hence, the averages of the results obtained with $W = 1.06$ and 1.1 were used to determine the difference between the images; with these, the accuracies are up to 94.82 and 90.98%, respectively.

Applying the same steps as with PSNR(Hw) to PSNR(Sw), the best weight was found to be $W = 1.04$. The scores shown in Table 11 were obtained with $W = 1.03$ and 1.05 , which are different from those used to obtain the results in Table 10 ($W = 1.07$ and 0.9). The weight of PSNR(Sw) is lower than that of PSNR(Hw). The best resulting average can reach up to 100 when using $W = 1.02$ and 1.04 . The results obtained with $W = 1.03$ and 1.05 are too close to that obtained with $W = 1.04$. Therefore, the averages of the results obtained with $W = 1.02$ and 1.06 were used to determine the difference; the accuracies are up to 99.26 and 97.93%, respectively.

Table 12 shows the best results for PSNR(Hw) for comparing dataset A with dataset B. Here, it is clearly evident that the optimal accuracy is different from that in Table 10. In contrast to the case of the original PSNR(H) value, the result is significantly improved. When using the original PSNR(H), the average score can only reach 57.4% at the highest. In contrast, with $W = 1.08$, the average accuracy score can reach as high as 98.52%.

Table 11
Scores obtained using PSNR(Sw) machine learning criteria.

Reference image	PSNR(Sw)									
	Dataset A compared	Dataset B compared								
	with dataset B ($W = 1.04$)	with dataset A ($W = 1.04$)	with dataset B ($W = 1.02$)	with dataset A ($W = 1.02$)	with dataset B ($W = 1.03$)	with dataset A ($W = 1.03$)	with dataset B ($W = 1.05$)	with dataset A ($W = 1.05$)	with dataset B ($W = 1.06$)	with dataset A ($W = 1.06$)
1M1	100	100	100	100	100	100	100	100	100	96.15
1M2	100	100	100	100	100	100	100	100	100	92.31
2M1	100	100	100	100	100	100	100	100	100	92.31
2M2	100	100	100	100	100	100	100	100	100	96.15
2M3	100	100	100	100	100	100	100	100	100	96.15
2L1.5	100	100	100	100	100	100	100	100	100	96.15
2L2.5	100	100	88.46	84.62	96.15	96.15	96.15	96.15	84.62	80.77
2R1.5	100	100	100	100	100	100	100	100	92.31	96.15
2R2.5	100	100	100	100	100	100	100	100	92.31	96.15
3M1	100	100	100	92.31	100	100	100	100	96.15	88.46
3M2	100	100	100	92.31	100	100	96.15	92.31	96.15	84.62
3M3	100	100	100	100	100	100	100	100	100	96.15
3L1.5	100	100	100	100	100	100	96.15	100	100	96.15
3L2.5	100	100	100	100	100	100	100	100	100	96.15
3R1.5	100	100	100	100	100	100	100	100	100	96.15
3R2.5	100	100	100	100	100	100	100	100	100	96.15
4M1	100	100	100	100	100	100	100	100	100	96.15
4M2	100	96.15	96.15	76.92	100	100	100	100	96.15	61.54
4M3	100	100	100	100	100	100	100	100	100	96.15
4L1.5	100	100	96.15	100	100	100	100	100	96.15	96.15
4L2.5	100	100	100	96.15	100	100	100	100	92.31	88.46
4R1.5	100	100	100	100	100	100	100	96.15	100	92.31
4R2.5	100	100	100	100	100	100	100	100	100	96.15
5M1	100	100	100	100	96.15	100	92.31	100	100	96.15
5M2	100	100	100	100	100	100	100	100	100	96.15
5M3	100	100	100	100	100	100	100	100	100	96.15
Average	100	99.85	99.26	97.78	99.7	99.85	99.26	99.41	97.93	92.75

Table 12
Score chart of machine learning PSNR(Hw) criteria.

Reference image	PSNR(Hw)			
	Dataset A compared with dataset B ($W = 1.0$)	Dataset A compared with dataset B ($W = 1.08$)	Dataset B compared with dataset A ($W = 1.0$)	Dataset B compared with dataset A ($W = 1.08$)
1M1	7.69	100	7.69	100
1M2	42.31	100	42.31	100
2M1	23.08	100	23.08	100
2M2	50	100	50	100
2M3	92.31	100	92.31	100
2L1.5	100	100	100	100
2L2.5	88.46	100	88.46	100
2R1.5	57.69	100	57.69	100
2R2.5	50	100	96.15	100
3M1	84.62	100	92.31	100
3M2	100	100	30.77	80.77
3M3	65.38	100	73.08	100
3L1.5	26.92	100	19.23	100
3L2.5	80.77	100	53.85	100
3R1.5	34.61	100	80.77	100
3R2.5	96.15	100	96.15	100
4M1	11.54	100	3.85	100
4M2	92.31	100	11.54	34.61
4M3	65.38	100	92.31	100
4L1.5	19.23	80.77	42.31	100
4L2.5	23.08	80.77	53.85	100
4R1.5	11.54	100	15.38	100
4R2.5	69.23	100	38.46	100
5M1	96.15	100	100	100
5M2	38.46	100	92.31	100
5M3	23.08	100	38.46	100
Average	55.77	98.52	57.4	96.75

Table 13 shows the best results for PSNR(Sw) for comparing dataset A with dataset B. Here, it is clearly evident that the optimal accuracy from Table 12 is different. As seen in Table 9, when using the original PSNR(S), the score can only reach 98.22%. When $W = 1.04$ is used, the accuracy can reach 100%.

By applying the same steps as with PSNR(Hw) and PSNR(Sw), we found the best weight using the SSIM(Hw, Sw, V) method to be $W = 1.02$. Referring back to Table 13 above, adding a weight when comparing the images results in an accuracy higher than that obtained without weight. Furthermore, the comparison accuracy does not continue to improve as the weight increases. After the accuracy reaches a certain value, it decreases as the weight increases further. Therefore, each method has its own optimal weight that gives the highest comparison accuracy. There is no single weight value that can result in the highest comparison accuracy for all the different methods.

The average accuracies obtained using the four different criteria are listed in Table 15. The proposed method⁽⁴¹⁾ had an accuracy of 32.69%. Considering the CPSNR(HSV), SSIM, and PSNR(V) methods, the average accuracy rate increased to 93.72, 91.94, and 83.58%, respectively. The use of the PSNR measurements of H and S layers resulted in improved accuracies of 56.59 and 98.00%, respectively. Compared with existing methods, the method proposed in this study yields a significant improvement. In addition, the results with machine

Table 13
Score chart of machine learning PSNR(Sw) criteria.

Reference image	PSNR(Sw)			
	Dataset A compared with dataset B ($W = 1.0$)	Dataset A compared with dataset B ($W = 1.04$)	Dataset A compared with dataset B ($W = 1.0$)	Dataset A compared with dataset B ($W = 1.04$)
1M1	100	100	100	100
1M2	100	100	100	100
2M1	100	100	100	100
2M2	100	100	100	100
2M3	100	100	100	100
2L1.5	100	100	100	100
2L2.5	84.62	100	84.62	100
2R1.5	100	100	100	100
2R2.5	92.31	100	100	100
3M1	96.15	100	92.31	100
3M2	96.15	100	92.31	100
3M3	100	100	100	100
3L1.5	100	100	100	100
3L2.5	100	100	100	100
3R1.5	100	100	100	100
3R2.5	100	100	100	100
4M1	100	100	100	100
4M2	96.15	100	76.92	96.15
4M3	100	100	100	100
4L1.5	96.15	100	100	100
4L2.5	92.31	100	96.15	100
4R1.5	100	100	100	100
4R2.5	100	100	100	100
5M1	100	100	100	100
5M2	100	100	100	100
5M3	100	100	100	100
Average	98.22	100	97.78	99.85

Table 14
Score of machine learning of SSIM(Hw, Sw, V) criteria.

Reference image	SSIM			
	Dataset A compared with dataset B ($W = 1.0$)	Dataset B compared with dataset A ($W = 1.02$)	Dataset B compared with dataset A ($W = 1.0$)	Dataset B compared with dataset A ($W = 1.02$)
1M1	73.08	92.31	73.08	92.31
1M2	73.08	100	73.08	92.31
2M1	88.46	100	88.46	96.15
2M2	100	100	100	100
2M3	92.31	88.46	92.31	96.15
2L1.5	100	100	100	100
2L2.5	57.69	92.31	57.69	80.77
2R1.5	96.15	61.54	96.15	100
2R2.5	57.69	69.23	96.15	100
3M1	92.31	100	92.31	96.15
3M2	96.15	100	53.85	73.08
3M3	92.31	100	92.31	100
3L1.5	100	100	100	100
3L2.5	100	100	100	100
3R1.5	76.92	88.46	100	100
3R2.5	100	100	100	100
4M1	53.85	80.77	61.54	88.46
4M2	88.46	100	30.77	46.15
4M3	80.77	96.15	100	100
4L1.5	26.92	26.92	96.15	100
4L2.5	53.85	73.08	96.15	100
4R1.5	80.77	88.46	96.15	100
4R2.5	100	100	61.54	84.62
5M1	92.31	100	100	100
5M2	61.54	92.31	100	100
5M3	73.08	84.62	100	100
Average	81.07	89.79	86.83	94.08

Table 15
(H, S, V) vs (Y, Cb, Cr)⁽³¹⁾. Accuracy results for four different criteria for shade matching.

	SCIELAB (Y,Cb,Cr) ⁽²⁷⁾	CPSNR (Y,Cb,Cr) ⁽²⁷⁾	Fuzzy Decision (Y,Cb,Cr) ⁽²⁷⁾	SCIELAB (H,S,V)	CPSNR (H,S,V)	Fuzzy Decision
Dataset A compared with dataset B	26.92%	30.77%	92.31%	87.28%	89.65%	84.91%
Dataset B compared with dataset A	38.46%	53.85%	92.31%	91.86%	91.43%	91.57%
Average	32.69%	42.31%	92.31%	89.57%	90.53%	88.24%

Table 16
Numbers of accurate shade matching pictures for different methods.

	SCIELAB (H,S,V)	CPSNR (H,S,V)	SSIM (H _w ,S _w ,V)	PSNR (H _w)	PSNR (S _w)	PSNR (V)	New Fuzzy Decision
Dataset A compared with dataset B	18	19	16	24	26	12	23
Dataset A compared with dataset B	22	20	21	23	25	13	24

Table 17
Average accuracies of four different criteria for shade matching.

Test image	This Work						
	SCIELAB (H,S,V)	CPSNR (H,S,V)	SSIM (H _w ,S _w ,V)	PSNR (H _w)	PSNR (S _w)	PSNR (V)	Fuzzy Decision
Dataset A compared with dataset B	87.28%	89.65%	84.91%	98.52%	100.00%	82.69%	98.96%
Dataset B compared with dataset A	91.86%	91.43%	91.57%	96.75%	99.85%	84.47%	99.56%
Average	89.57%	90.53%	88.24%	97.64%	99.93%	83.58%	99.26%

learning in each colorimetric calculation also improved the scores for PSNR(H) and PSNR(S) to 97.64 and 99.93%, respectively. As for the fuzzy decision method, the proposed method showed the best performance with 100% accuracy.

In Tables 12–15, the differences in scores are due to adding the different weighting coefficients after adding PSNR(H) and PSNR(S). Moreover, Table 15 shows the results of the comparison of dataset B with dataset A. Testing is repeated with all the methods and the results are listed accordingly. Here, dataset B is used as the reference for comparing dataset A, and Table 16 shows the results when dataset A was used as the reference. The results of the two comparison modes are averaged, as shown in Table 17.

5. Conclusions

The S-CIELAB index combines luminance, red–green positions, and yellow–blue positions into one index. In addition to using a mixed index (including luminance and color information), 26 dental shadow tabs were classified into the two dimensions of luminance and chroma for selecting a color space. Therefore, using the indexes PSNR(H), PSNR(S), and PSNR(V) increased the accuracy of shadow matching because the focus of the proposed method is on one color space of the image without affecting the information in the other color spaces.

As shown in Table 13, the average score of S-CIELAB (H, S, V) was 94.53%. For CPSNR (H, S, V), the average score increased to 93.72%, as shown in Table 3. The average scores were significantly improved to 97.64 and 99.93% by using PSNR(Hw) and PSNR(Sw), respectively, as shown in Tables 7 and 8.

Finally, the proposed fuzzy decision was found to show the best performance, with an average score of 99.26%, as shown in Table 8. The use of the H and S image layers for tooth color matching together with the proposed fuzzy decision making method yielded excellent results compared with the other methods.

References

- 1 A. Mittal, D. Kumar, M. Mittal, T. Saba, I. Abunadi, A. Rehman, and S. Roy: *Sensors* **20** (2020) 1068. <https://doi.org/10.3390/s20041068>
- 2 E. B. Torres, C. Caballero, and S. Mistry: *Sensors* **20** (2020) 2. <https://www.ncbi.nlm.nih.gov/pmc/articles/PMC7014496/>
- 3 S. Jiang, H. Qi, J. Zhang, S. Zhang, R. Xu, Y. Liu, L. Meng, and D. Ming: *Sensors* **19** (2019) 24. <https://www.ncbi.nlm.nih.gov/pmc/articles/PMC6960671/>
- 4 A. AlShibli and H. Mathkour: *Sensors* **19** (2019) 19. <https://www.ncbi.nlm.nih.gov/pmc/articles/PMC6806227/>
- 5 Y. Yang, M. Zhu, Y. Wang, H. Yang, Y. Wu, and B. Li: *Sensors* **19** (2019) 19. <https://www.ncbi.nlm.nih.gov/pmc/articles/PMC6806596/>
- 6 Justiawan, R. Sigit, Z. Arief, and D. A. Wahjuningrum: *J. Dentomaxillofacial Sci.* **2** (2017) 95. <https://doi.org/10.15562/jdmfs.v2i2.525>
- 7 J. Yang, Y. Xie, L. Liu, B. Xia, Z. Cao, and C. Guo: 2018 IEEE 42nd Annu. Computer Software and Applications Conf. (COMPSAC) (2018) 23. <https://ieeexplore.ieee.org/stamp/stamp.jsp?tp=&arnumber=8377701>
- 8 H. Chen, K. Zhang, P. Lyu, H. Li, L. Zhang, J. Wu, and C. H. Lee: *Sci. Rep.* **9** (2019) 3840. <https://www.nature.com/articles/s41598-019-40414-y>
- 9 J. M. Guo, C. H. Hsia, K. Wong, J. Y. Wu, Y. T. Wu, and N. J. Wang: *IEEE Trans. Veh. Technol.* **65** (2016) 6. <https://ieeexplore.ieee.org/stamp/stamp.jsp?tp=&arnumber=7353207>
- 10 W. Yang, S. Wang, J. Hu, G. Zheng, J. Yang, and C. Valli: *IEEE Trans. Ind. Inf.* **15** (2019) 7. <https://ieeexplore.ieee.org/stamp/stamp.jsp?tp=&arnumber=8648285>
- 11 Q. Zhang, Y. Liu, H. Han, J. Shi, and W. Wang: *IEEE Access* **6** (2018) 60605. <https://ieeexplore.ieee.org/stamp/stamp.jsp?tp=&arnumber=8490220>
- 12 C. H. Hsia: *IEEE Sens. J.* **18** (2018) 2. <https://ieeexplore.ieee.org/stamp/stamp.jsp?tp=&arnumber=8105785>
- 13 Y. K. Lee, B. Yu, J. I. Lim, and H. N. Lim: *J. Prosthetic Dent.* **105** (2011) 9. [https://doi.org/10.1016/S0022-3913\(11\)60006-1](https://doi.org/10.1016/S0022-3913(11)60006-1)
- 14 R. D. Paravina, J. M. Powers, and R. M. Fay: *Int. J. Prosthodont.* **15** (2002) 73. <https://pubmed.ncbi.nlm.nih.gov/11887603>
- 15 R. C. Sproull: *J. Prosthetic Dent.* **29** (1973) 556. [https://doi.org/10.1016/0022-3913\(73\)90036-X](https://doi.org/10.1016/0022-3913(73)90036-X)
- 16 VITA: VITA classical A1–D4 shade guide, <https://paylessdentalsupplies.com/product/vita-classical/> (Picture reference 1).
- 17 VITA: Vita Zahnfabrik, <https://www.vita-zahnfabrik.com/en/History-67.print> (Picture reference 2).
- 18 VITA: VITA Toothguide 3D-MASTER, <https://www.vita-zahnfabrik.com/en/VITA-Toothguide-3D-MASTER-26230,27568.html>
- 19 M. Alomari and R. G. Chadwick: *Br. Dent. J.* **211** (2011) 1. <https://www.nature.com/articles/sj.bdj.2011.1006.pdf>
- 20 T. L. Shih: *Dent. Technol. Mag.* **16** (2017) 11.
- 21 R. G. Kuehni and R. T. Marcus: *Color Res. Appl.* **4** (1979) 83. <https://onlinelibrary.wiley.com/doi/epdf/10.1111/j.1520-6378.1979.tb00094.x>
- 22 R. D. Paravina: *J. Dent.* **37** (2009) 15. <https://doi.org/10.1016/j.jdent.2009.02.005>
- 23 S. J. Chu, R. D. Trushkowsky, and R. D. Paravina: *J. Dent.* **38** (2010) 2. <https://doi.org/10.1016/j.jdent.2010.07.001>
- 24 W. K. Tam and H. J. Lee: *J. Dent.* **40** (2012) 3. <https://doi.org/10.1016/j.jdent.2012.06.004>
- 25 S. L. Wang, W. T. Wang, and F. Wu: 2011 4th Int. Conf. Biomed. Eng. Inf. (BMEI) **4** (2011) 1950. <https://ieeexplore.ieee.org/stamp/stamp.jsp?tp=&arnumber=6098746>

- 26 K. Pahwa and N. Agarwal: 2019 Int. Conf. Machine Learning Big Data, Cloud and Parallel Computing (COMITCon) (2019). <https://doi.org/10.1109/COMITCon.2019.8862225>
- 27 O. E. Pecho, R. Ghinea, R. Alessandretti, M. M. Pérez, and A. B. Della: Dent. Mater. **32** (2016) 82. <https://doi.org/10.1016/j.dental.2015.10.015>
- 28 E. Mendi and C. Bayrak: 2010 IEEE 39th Applied Imagery Pattern Recognition Workshop (AIPR) **29** (2011) 1. <https://doi.org/10.1109/AIPR.2010.5759680>
- 29 D. C. Montgomery, E. A. Peck, and G. G. Vining: Introduction to Linear Regression Analysis (John Wiley & Sons, Inc., New Jersey, 2012) 5th ed.
- 30 N. R. Draper and H. Smith: Applied Regression Analysis (Springer-Verlag, New York, 1998) 3rd ed.
- 31 T. L. Lin, C. H. Chuang, S. L. Chen, N. H. Lin, S. G. Miaou, S. Y. Lin, C. A. Chen, H. W. Liu, and J. F. Villaverde: J. Intell. Fuzzy Syst. **36** (2019) 1133. <https://doi.org/10.3233/JIFS-169887>
- 32 S. L. Wang, W. T. Wang, and F. Wu: Int. Biomedical Engineering and Informatics Conf. (BMEI) **4** (2011) 1950. <https://doi.org/10.1109/BMEI.2011.6098746>
- 33 A. G. Wee, D. T. Lindsey, S. Kuo, and W. M. Johnston: Dent. Mater. **22** (2006) 553. <https://doi.org/10.1016/j.dental.2005.05.011>
- 34 S. Ishikawa-Nagai, K. Ishibashi, O. Tsuruta, and H. P. Weber: J. Prosthetic Dent. **93** (2005) 129. <https://doi.org/10.1016/j.prosdent.2004.10.024>
- 35 X. Zhang and B. A. Wandell: J. Soc. Inf. Display **5** (2012) 61. <https://doi.org/10.1889/1.1985127>
- 36 J. Wu, M. Anisetti, W. Wu, E. Damiani, and G. Jeon: IEEE Trans. Image Process. **25** (2016) 5369. <https://ieeexplore.ieee.org/stamp/stamp.jsp?tp=&arnumber=7556279>
- 37 A. T. Nasrabadi, M. A. Shirsavar, A. Ebrahimi, and M. Ghanbari: 2014 IEEE Int. Symp. Broadband Multimedia Systems and Broadcasting (2014) 1. <https://ieeexplore.ieee.org/stamp/stamp.jsp?tp=&arnumber=6873482>
- 38 K. L. Chung, C. C. Huang, and T. C. Hsu: IEEE Trans. Image Process. **26** (2017) 12. <https://ieeexplore.ieee.org/stamp/stamp.jsp?tp=&arnumber=8025573>
- 39 M. A. Hassan and M. S. Bashraheel: 2017 8th Int. Conf. Information Technology (ICIT) **23** (2017) 691. <https://ieeexplore.ieee.org/stamp/stamp.jsp?tp=&arnumber=8079929>
- 40 A. Kavousi-Fard, A. Khosravi, and S. Nahavandi: IEEE Trans. Power Syst. **31** (2016) 18. <https://ieeexplore.ieee.org/stamp/stamp.jsp?tp=&arnumber=7035120>
- 41 K. Gulzard, J. Sang, M. Ramzan, and M. Kashif: IEEE Access **5** (2017) 13570. <https://ieeexplore.ieee.org/stamp/stamp.jsp?tp=&arnumber=7973147>
- 42 S. L. Chen: IEEE Access. **3** (2015) 743. <https://ieeexplore.ieee.org/stamp/stamp.jsp?tp=&arnumber=7113779>
- 43 K. L. Lo, Y. J. Lin, and W. H. Siew: IEEE Proc. **146** (1999) 276. <https://ieeexplore.ieee.org/stamp/stamp.jsp?tp=&arnumber=818084>
- 44 S. Taneja, B. Suri, and H. Narwal: 2016 6th Int. Conf. Cloud System and Big Data Engineering (Confluence) (2016). <https://doi.org/10.1109/CONFLUENCE.2016.7508041>